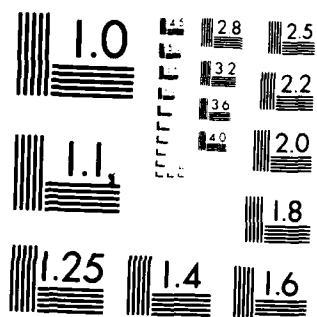END
DATE
FILMED
8 83
DTIC
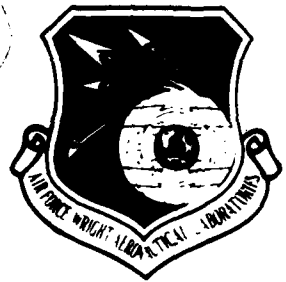
MICROCOPY RESOLUTION TEST CHART

NATIONAL BUREAU OF STANDARDS 1963-A

AFWAL-TR-83-4006

CREEP CRACK-OPENING DISPLACEMENT MEASUREMENTS IN IN-I00

AT 732 C

William N. Sharpe, Jr.
Louisiana State University
Baton Rouge, LA 70803

March 1983

Interim Report for Period September 1978 - March 1983

Approved for public release; distribution unlimited.

MATERIALS LABORATORY
AIR FORCE WRIGHT AERONAUTICAL LABORATORIES
AIR FORCE SYSTEMS COMMAND
WRIGHT-PATTERSON AIR FORCE BASE, OHIO 45433

JUL 2 6 1983

A

83 07 26 149

GORDON ATKINS
Metals Behavior Branch
Metals and Ceramics Division

JOHN P. HENDERSON, Chief
Metals Behavior Branch
Metals and Ceramics Division

FOR THE COMMANDER

LAWRENCE N. HJELM, Asst Chief
Metals and Ceramics Division
Materials Laboratory

REPORT DOCUMENTATION PAGE

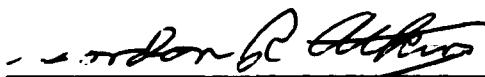**READ INSTRUCTIONS BEFORE COMPLETING FORM**

1. REPORT NUMBER	2. GOVT ACCESSION NO.	3. RECIPIENT'S CATALOG NUMBER
AFWAL-TR-83-4006	AD-A130675	

4. TITLE (and Subtitle)

Creep Crack-Opening Displacement Measurements in IN-100 at 732 C

5. TYPE OF REPORT & PERIOD COVERED

INTERIM Sep 78 - March 83

6. PERFORMING ORG. REPORT NUMBER

7. AUTHOR(s)

William N. Sharpe, Jr.

8. CONTRACT OR GRANT NUMBER(s)

F33615-81-K-5014

9. PERFORMING ORGANIZATION NAME AND ADDRESS

Louisiana State University
Baton Rouge, LA 70803

10. PROGRAM ELEMENT, PROJECT, TASK AREA & WORK UNIT NUMBERS

ILIR0139; 61101F*

11. CONTROLLING OFFICE NAME AND ADDRESS

Materials Laboratory (AFWAL/MLLN)
Air Force Wright Aeronautical Laboratories (AFSC)
Wright-Patterson Air Force Base, Ohio 45433

12. REPORT DATE

March 1983

13. NUMBER OF PAGES

48

14. MONITORING AGENCY NAME & ADDRESS(if different from Controlling Office)

15. SECURITY CLASS. (of this report)

Unclassified

15a. DECLASSIFICATION/DOWNGRADING SCHEDULE

16. DISTRIBUTION STATEMENT (of this Report)

Approved for public release; distribution unlimited.

17. DISTRIBUTION STATEMENT (of the abstract entered in Block 20, if different from Report)

18. SUPPLEMENTARY NOTES

*This research was partially funded by the In-House Independent Research Fund.

19. KEY WORDS (Continue on reverse side if necessary and identify by block number)

Creep Crack Growth
Crack Opening
IN-100
Interferometric
Displacement Gage
Nickel-Based Superalloy

20. ABSTRACT (Continue on reverse side if necessary and identify by block number)

Creep crack-opening displacemnt was measured at 732 C (1350 F) using an interference displacement gage and a minicomputer based analysis system to calculate compliance and provide realtime control and analysis. The system, based on a HeNe laser interferometer, was used to measure creep crack growth in IN-100, a nickel-based superalloy.

DD FORM 1 JAN 73 **1473** EDITION OF 1 NOV 65 IS OBSOLETE
S/N 0102-LF-014-6601

TABLE OF CONTENTS

iii

INTRODUCTION

The classical method of measuring fatigue crack growth in a specimen under fatigue or creep conditions is observation of the crack tip with a low-power travelling microscope. A commerically available technique uses a foil gage whose resistance "legs" break as the crack advances. Other techniques such as the electropotential method and various compliance methods actually make an indirect measurement of the crack length, relating either the voltage drop or the slope of the compliance curve to the crack length. Another approach is to make displacement measurements at some point on the specimen and use a finite-element computer code to relate these displacements to the crack length; this approach is referred to as the Hybrid Experimental-Numerical (HEN) approach. With the mature state of finite-element analysis of linear elastic problems, this later approach is quite effective. However, when one becomes interested in material behavior at elevated temperatures, the HEN approach becomes more difficult for two reasons: difficulty in displacement measurements and the necessity to incorporate the nonlinear behavior of the material into the finite element code. This report addresses the first of these difficulties - displacement measurements.

Displacement measurements at temperatures on the order of 700-760 C are difficult at best, and yet this is a reasonable temperature range for components such as jet engine turbine disks. The most common displacement measurement method is to attach quartz rods to the specimen, transferring the motion to a cooler region where a LVDT or strain gage-based displacement transducer is used. This technique provides a convenient analog signal, but is quite bulky and somewhat limited in sensitivity. Capacitance gages are also candidates for high temperature measurement, but tend to be expensive.

This paper describes an application of the interferometric strain displacement gage (ISDG) to high temperature creep and compliance measurements on a particular superalloy, IN-100. The principal features of the ISDG for this type of measurements are: extremely short gage length permitting displacement measurements near the crack, good long-term stability, and reasonable sensitivity. The particular setup described here is especially simple and inexpensive.

The basis of the ISDG are first described very briefly. The experimental techniques are next presented, followed by a description of the IN-100 specimens tested. Results fall into two categories: PHASE I in which the compliance data was obtained from stripchart records and PHASE II in which a minicomputer was used for experiment control and data acquisition. A major consideration in the two RESULTS sections is the documentation of the displacement behavior under various creep loads for use by subsequent researchers.

1

EXPERIMENTAL TECHNIQUES

The ISDG is a laser-based displacement measuring system with interferometry as its underlying principle. It measures the relative displacement between two tiny reflecting indentations placed on the surface of a specimen. The basics of the ISDG are described in Reference 1, so only a very brief explanation will be given here.
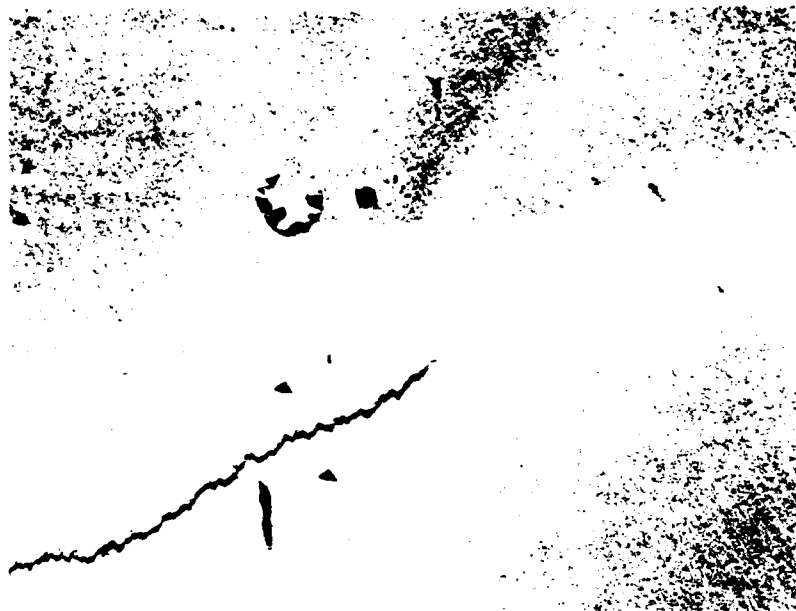
Figure 1. SEM photograph of a pair of indentations astride a crack. This was taken after exposure to 732°C for two hours. The indentations are approximately 25 microns on a side and are 100 microns apart.

Figure 1 is a photomicrograph of two indentations placed astride a fatigue crack. These pyramidal indentations are easily applied with a Vicker's hardness tester. Typically they are 25 microns square and 10 microns deep and are spaced 50-150 microns apart. The primary optical requirements of the indentations are that they be reflective to an incident laser beam and small enough to cause appreciable diffraction of that beam.

When illuminated by the coherent monochromatic radiation of a laser, the reflecting sides of the two indentations produce interference fringe patterns in space. Four fringe patterns are produced, one emanating from each of the four sides of the indentations. Only the two patterns from the sides parallel to the fatigue crack are of interest. If one monitors the motions of these two fringe patterns, the relative displacement between the two indentations can be measured. The relations between displacement, δd, and fringe motion is:

$$\delta d = \frac{\delta m_1 + \delta m_2}{2} \frac{\lambda}{\sin \alpha_o} \qquad (1)$$

λ is the wave length of light, α_o is the angle between the incident laser beam and the central portion of the fringe pattern, and δm_1 and δm_2 are the fringe motions expressed as a fraction of the fringe spacing. The averaging of the two fringe pattern motions eliminates the effect of rigid-body translation parallel to the displacement direction. Using typical values of $\lambda = 0.6328$ micron and $\alpha_o = 42$ degrees, one complete fringe shift corresponds to a displacement of 0.95 microns.

Figure 2 is a schematic of the experimental setup. The actual arrangement has a small servocontrolled mirror in the optical path of each fringe pattern. This mirror is used to adjust the fringe pattern to either a maxima or a minima once the creep load is reached. Although not really necessary, the mirror makes the strip-chart record easier to read.
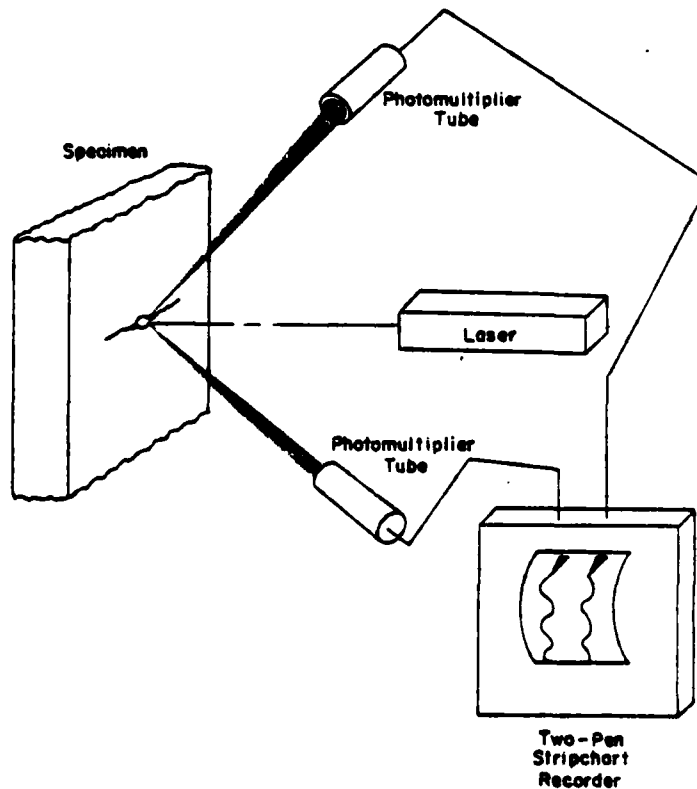
Figure 2.   Schematic of the displacement measurement system.

The He-Ne laser used for these tests is a 5 milliwatt Spectra Physics Model 120. The fringe-sensing devices are Amperex XP1117 photomultiplier tubes covered by an interference filter and a thin slit that is narrower than the spacing between fringes. Photoresistive devices are quite adequate for this application (see Reference 2), although one has to pay attention to their frequency response. As Figure 2 indicates, the signals from the two photomultiplier tubes are fed to an ordinary strip chart recorder. A portion of a typical creep record is shown in Figure 3.
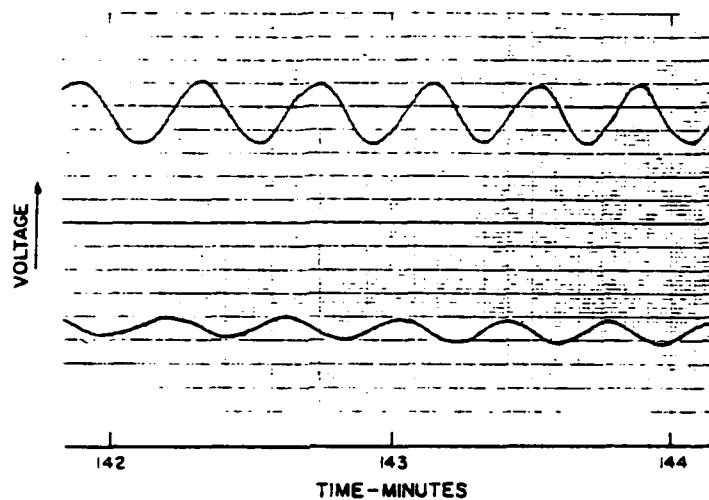
Figure 3.   Typical stripchart record. The different amplitudes are caused by the gain settings.

An MTS 90 kilonewton electrohydraulic testing machine was used to load the specimens. They were heated with a special resistance furnace constructed locally. The furnace has three quartz ports for the entering laser beam and the two fringe patterns. It took approximately 1 hour for the furnace to reach 732 C.

The data analysis is very simple. One simply records the times at which maxima and minima occur on each of the traces in Figure 3. Each maxima or minima corresponds to a fringe increment of ½ in Equation 1. The fringe increments versus time are plotted for both the upper and lower fringe pattern, and the final displacement is determined by averaging the two curves as a function of time. After multiplying by the appropriate calibration constant, the final result is a plot of displacement versus time as shown in Figure 4.

4
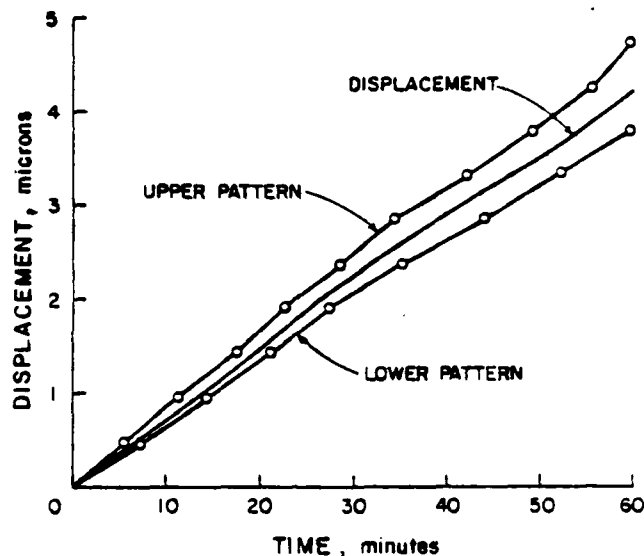
Figure 4.   Typical displacement record. From Test 5.

Compliances are measured by decreasing the load from the creep load
to some smaller value and then reloading. The main difference between
the PHASE I and PHASE II results is in how this was accomplished. In
PHASE I, the compliance load signal was generated by the digital signal
generator associated with the test machine and the fringe motion re-
corded on the stripchart. In PHASE II, the load signal was generated
and the fringe motion recorded by a minicomputer. A Digital Equipment
Corporation MINC minicomputer with 64 K-byte random access memory and
twin floppy disks was used. It has 4 D/A and 16 A/D convertors (both
expandable) and graphics capability.

λ in Equation 1 is known   precisely, but it is estimated that
the relative uncertainty in sin α_o is $\pm$ 1 percent. There is some judg-
ment required in locating a max or a min as the records are read; this
is estimated to lead to a relative uncertainty of $\pm$ 2 percent. A rela-
tive displacement measurement then has a relative uncertainty of $\pm$ 3
percent. This is the simplest version of an ISDG system. It has a
resolution of approximately 1/8 micron. A more sophisticated,
minicomputer-based system is described in reference 3.

In some of the tests in Phase I (Nos. 8 and 12a), the stress inten-
sity factor was small enough that the creep displacement was not more
than 1 micron. A different approach for relative displacement meas-
urement was used in these cases. A sawtooth function generator drove
the two servocontrolled mirrors which generated a linear sweep of the
fringe pattern across the slitted PMT. The PMT signals were recorded on
the stripchart recorder and were in effect a "snapshot" of the position
of the fringes relative to the start of the sweep. The sweep rate was
0.04 hz, and three fringes were usually covered. Relative fringe motion

5

was measured between successive sweeps - giving a resolution of approximately 1/20 of the fringe spacing. This procedure was not employed in any of the compliance measurements.

The principal advantages of the ISDG for the measurements described here are its small size, lack of mechanical contact with the specimen, and a measurement scheme based on relative amplitudes of the optical (or electrical) signal which enable stability of long-term measurements. The simple techniques used for this particular series of high temperature measurements are described in the following section.

MATERIAL AND SPECIMENS

The material was the nickel-based superalloy, IN-100. The specimens had the center-cracked geometry with a width of 25 mm and a thickness of 7.6 mm. The test section was 40 mm long, and the circular grip ends were threaded. A starter notch was electromachined through the center of the specimen and fatigue cracks grown from each edge of that starter notch to an initial length of approximately 3 mm. There was no particular difficulty in attaining uniform lengths of the two cracks on both sides of the specimen. The initial fatigue cracks were grown at room temperature with a final K of 16.3 MPa-m$^{\frac{1}{2}}$. Figure 5 is a schematic of the crack in the specimen; the four dimensions are all measured from the specimen centerline and are listed in the RESULTS sections for each test.
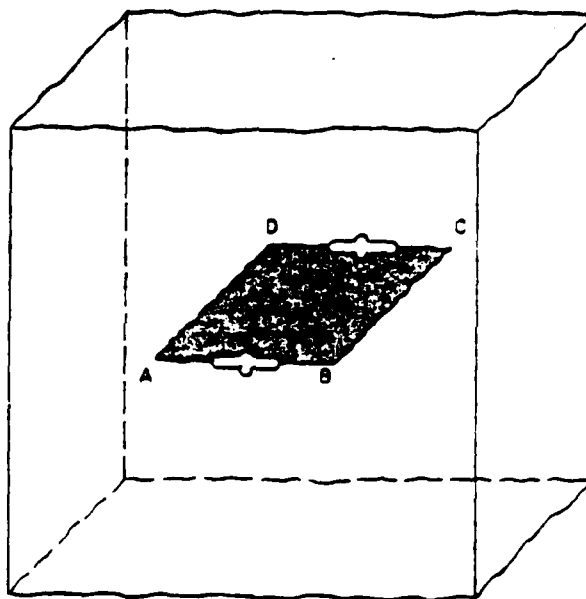
Figure 5.   Diagram denoting crack lengths.

The critical aspect of high temperature testing with the ISDG is that the specimen surface remains reflective at temperature. The indentations on a brightly polished IN-100 specimen placed in a closed resistance furnace will deteriorate at approximately 600 C. Previous experimentation with IN-100 had shown that if a specimen was heated to the test temperature of 732 C in an r-f furnace for 1 hour, a thin bluish oxide film forms on the surface which protects it from further degradation at the test temperature in a closed resistance furnace. The operating procedure is to pretreat the specimens in an r-f furnace, apply the indentations, and then test. Our supposition is that a much finer oxide film is formed in the r-f furnace with its continual flow of air past the heated specimen. This little bit of witchcraft works very

successfully every time; in fact, the fringe patterns from the indentation become slightly brighter at test temperature, indicating the oxide film has a higher reflectance at that temperature. The photomicrograph of Figure 1 was taken after the specimen had been exposed to the test temperature of 732 C for approximately 2 hours.

PHASE I RESULTS

In this first series of tests, all fringe motions were recorded on the stripchart recorder as indicated in Figure 2. The first four tests recorded only load-displacement during loading, creep displacement at maximum load, and load-displacement during unloading. Compliance measurements were made at various temperatures as the specimen heated up by loading from zero load to less than half the maximum load and then immediately unloading. Loading and unloading was accomplished via the MTS digital function generator and typically took 10 seconds or less.

The last three tests in this series added compliance tests interspersed with the creep data. This was also accomplished via the digital function generator. The specimen was manually loaded via the set point to a load less than the maximum load (typically 17.8 kN less). Then the stripchart was turned on at 100 mm/sec and the "start" button of the MTS pushed. The test machine stopped automatically at the maximum load. The stripchart was then slowed to 5 mm/sec and creep fringe motion recorded. When a compliance was desired, "return to zero" was pushed on the MTS which unloaded the specimen back to the manually set load; it was immediately returned to the maximum load by pushing the "start" button. Each compliance took approximately 10 seconds, and the stripchart recorder was speeded up for the measurement. No significant differences were observed for the loading and unloading behavior.

Test Number - 5

Specimen Number - 2

Crack Length (mm)	
A	3.43
B	3.05
C	2.77
D	3.58

Creep Load (kN) - 44.9

Compliance Increment (kN) - 0

Stress Intensity Factor (MPa-m$^{\frac{1}{2}}$) - 25.3

Temperature (C) - 718

Test Duration - 1 hour

ISDG Location - 35 microns behind tip of crack A.

The creep results for this test are given earlier in Figure 4. A telescope was set up to observe the crack during creep - the laser was turned off for the 20 seconds or so it took to make an observation. One

9

side of a "feather" of considerable deformation was observed ahead the crack tip soon after the creep load was applied. During the course of the 60 minute test, another "feather" grew ahead of the tip. Post-test examination showed this "feathered" region to be symmetric and to extend approximately 125 microns ahead of the original crack tip. There was considerable grain boundary separation observed in the region between the two "feathers." The creep load corresponding to 25.3 MPam$^{\frac{1}{2}}$ on this specimen leads to a moderate short-term creep growth.

Test Number - 6

Specimen Number - 2 (precracked at room temperature after Test 5)

Crack Length (mm)	
A	4.78
B	4.98
C	4.39
D	4.67

Creep Load (kN) - 36.3   Compliance Increment (kN) - 36.3 to 18.5

Stress Intensity Factor (MPa-m$^{\frac{1}{2}}$) - 25.3   Temperature (C) - 721

Test Duration - 1 hour

ISDG Location(s) - 112 microns behind tip of crack A (4.67 mm from centerline), 3.33 mm and 2.03 mm from centerline.

Figure 6 is a plot of compliances taken at various temperatures as the specimen heated up. These were taken at the middle set of indents, but similar behavior was recorded at the other positions.

Figure 7 shows displacement at the tip versus time as the specimen was loaded. The creep behavior is shown in Figure 8. Telescope observations showed the first "feather" to appear immediately upon loading. Because of this observation, the creep displacement measurement wasn't started until 5 minutes after the test started. Figure 8 shows a slightly higher slope than Figure 4; these were identical tests, but the indents were slightly farther back from the tip here. Figure 9 shows the displacement during unloading - taking zero at the maximum load. these last three figures are consistent - showing approximately 8 microns displacement during loading, 5 microns creep, and 12 microns unloading.
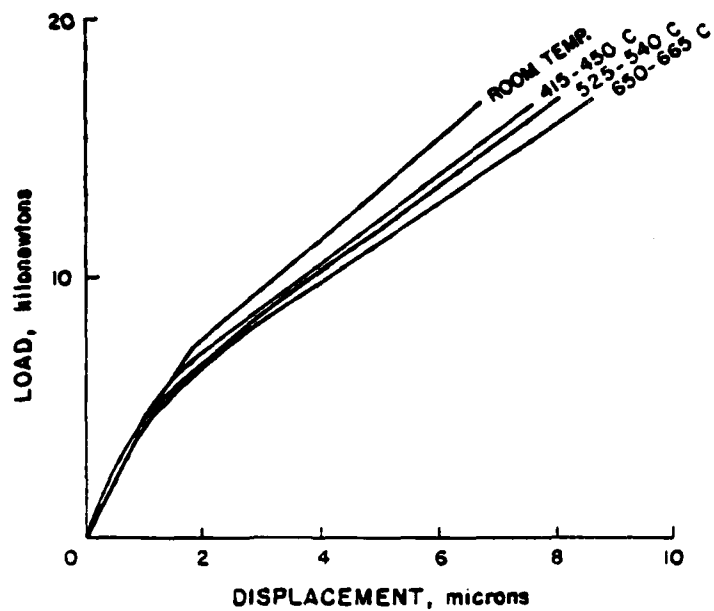
Figure 6.   Compliance at various temperatures for Test 6.
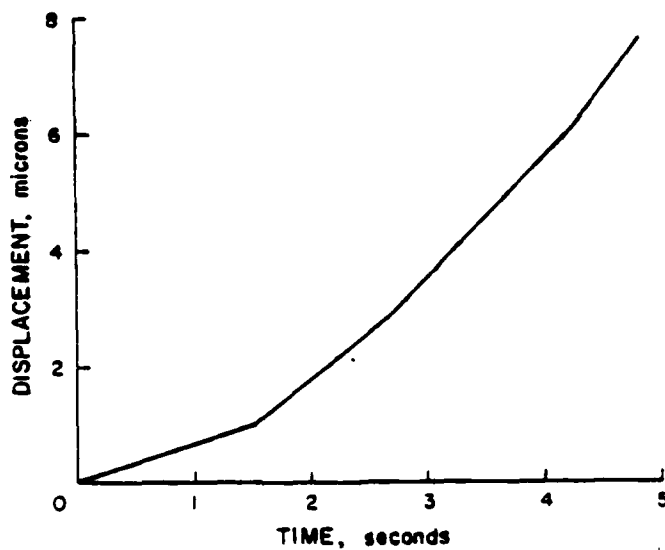
Figure 7.   Displacement-time as the specimen of Test 6 was loaded to
                 its creep load of 36.3 kN from 18.5 kN.

11
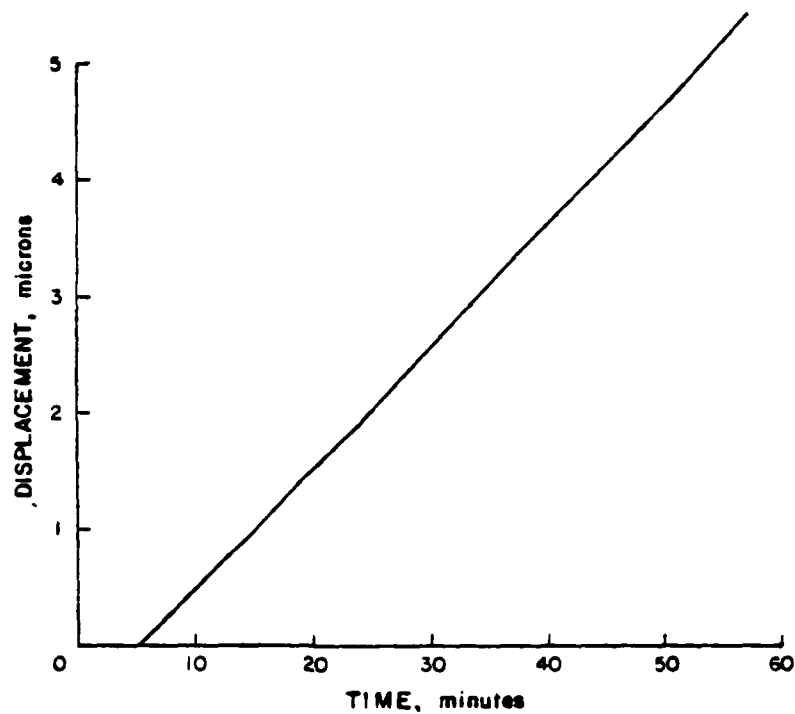
Figure 8.   Creep displacement for Test 6. Note the displacement
             measurement was not started until 5 minutes after load
             was applied because of telescope measurements.
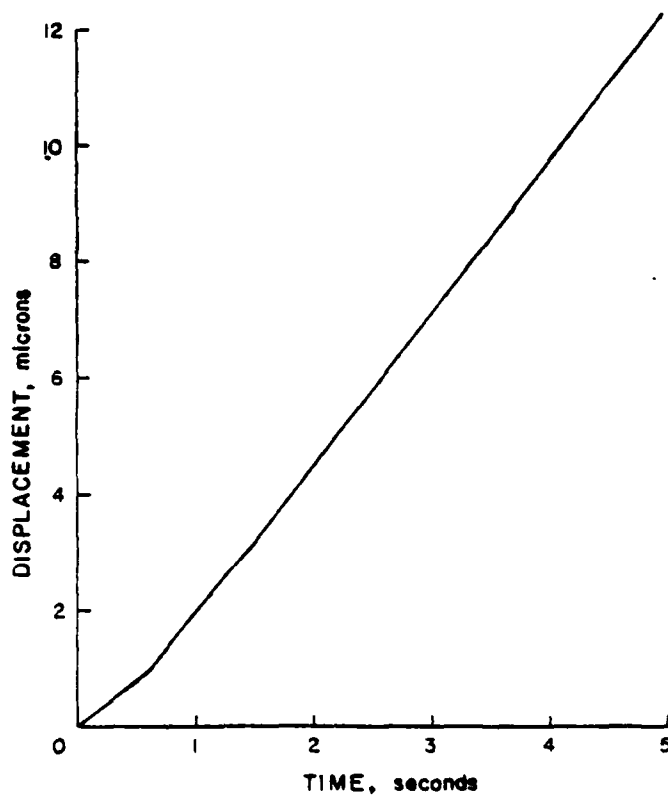
Figure 9.   Unloading displacement-time for Test 6.

Specimen Number - 3

Crack Length (mm)	
A	3.25
B	3.07
C	3.10
D	3.33

Creep Load (kN) - 47.6   Compliance Increment (kN) - 47.6 to 25.4

Stress Intensity Factor (MPa-$m^{\frac{1}{2}}$) - 25.3   Temperature (C) - 716

Test Duration - ~ 15 minutes

ISDG Location(s) - 104 microns ahead of crack C tip and 2.13 mm from
    centerline.

   This was an unsuccessful attempt to measure strain ahead of the
crack tip. Figure 10 is a scanning electron micrograph of the specimen
after test. The plastic zone spreads out in a "Y" configuration from
the tip upon reaching the maximum load. This does not cause the indents
to become non-reflective, but it does rotate them with respect to each
other so that no interference fringes occur.

   Compliance measurements were made at various temperatures but are
not included.

Figure 10.   SEM photograph of the region ahead of the crack tip after Test 7. The indentations are 100 microns apart.

Specimen Number - 5

	Crack Length (mm)
A	3.28
B	3.05
C	3.12
D	3.18

Creep Load (kN) - 31.6, 37.9, 43.2, 48.5

Compliance Increment (kN) - 15.6

Stress Intensity Factor (MPa-m$^{\frac{1}{2}}$) - 16.5, 19.8, 22.5, 25.3

Temperature (C) - 716

Test Duration - 60, 30, 30, 30 minutes

ISDG Location(s) - 164 microns behind crack tip B and 1.73 mm from centerline.

These four tests were run sequentially on the same specimen after it reached temperature. The first test was run for 60 minutes, and the latter three for 30 minutes each. The specimen was unloaded between tests and reloaded to the creep load - this operation took less than 1 minute. Figure 11 portrays the creep behavior at each load. It is important to recognize the potential effect of previous history on the latter three experiments. Note that test 8d at 25.3 MPa-m$^{\frac{1}{2}}$ shows a much lower creep rate than either test 5 or 6, and the indents were even further behind the tip. Note also that the displacement curves have a higher slope initially.

Compliance curves were recorded at various temperatures but are not reported.
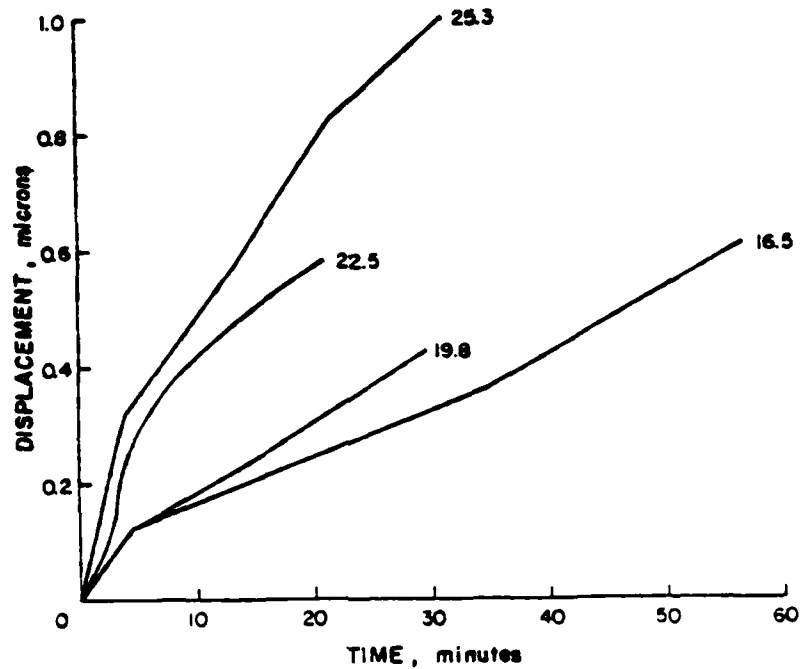
Figure 11. Creep curves for Test 8 at various stress intensity factors - MPa-m$^{\frac{1}{2}}$.

Test Number - 9

Specimen Number - 4

Crack Length (mm)	
A	3.15
B	3.10
C	3.08
D	3.30

Creep Load (kN) - 71.5   Compliance Increment (kN) - 71.5 to 35.6

Stress Intensity Factor (MPa-m$^{\frac{1}{2}}$) - 38.5   Temperature (C) - 710

Test Duration - 1 hour

ISDG Location(s) - 120 microns behind crack tip A and 1.35 mm from centerline.

17

This was a creep test at high K with compliances interspersed at 20 minute intervals. A major difference here is that creep and compliance measurements were made at the indents nearest the centerline - not at the tip.

Figure 12 shows the large amount of creep recorded near the centerline, and Figure 13 shows the compliances at various times. Note that the compliance is smaller than that measured on the initial loading for quite a while after creep has started.

Tests 10 and 11 were unsuccessful because of equipment or procedural malfunction.
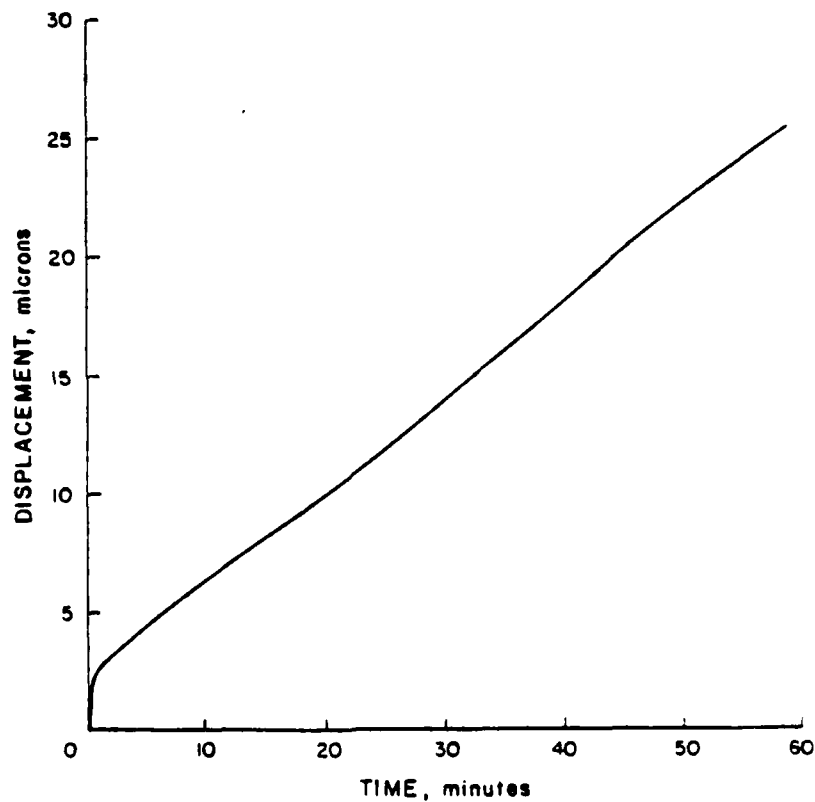
Figure 12.   Creep near the center of the specimen for Test 9.
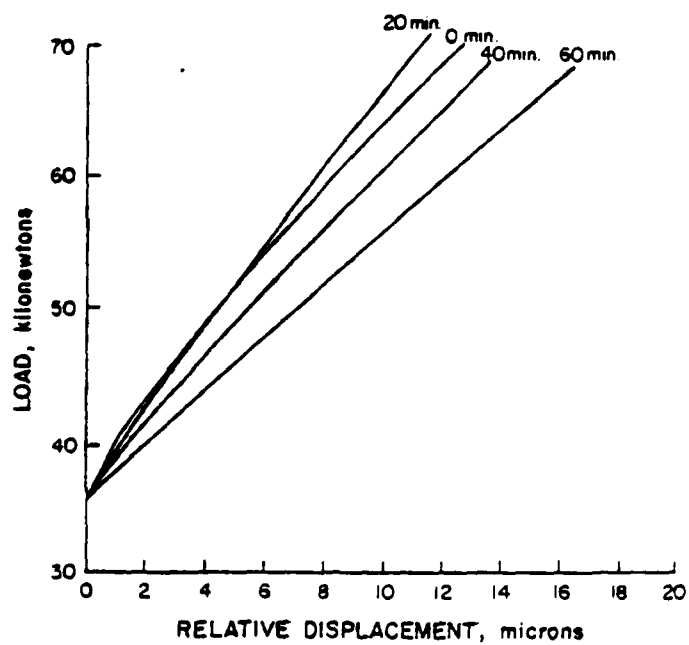
Figure 13.   Compliance curves at various times for Test 9.

<u>Test Number</u> - <u>12a, b, c</u>

Specimen Number - 3 (precracked at room temperature after Test 7)

<u>Crack Length (mm)</u>

A   4.93

B   5.11

C   4.65

D   4.24

Creep Load (kN) - 23.1, 34.1, 50.0

Compliance Increment (kN) -

Stress Intensity Factor (MPa-m$^{\frac{1}{2}}$) - 16.5, ~ 25.3, ~ 38.5

Temperature (C) - 727

Test Duration - 30 minutes at each load

ISDG Location - 1.50 mm from centerline along crack B.

The specimen was loaded to K = 16.5 MPa-m$^{\frac{1}{2}}$ and held there for 30 minutes. The loading and unloading compliances are given in Figure 14 with the creep plotted in Figure 15.
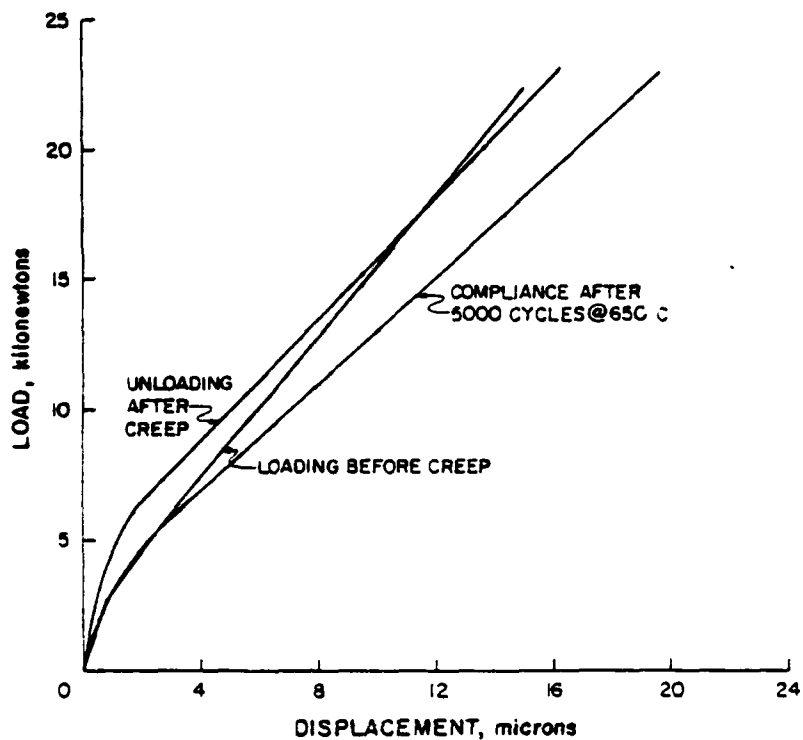
Figure 14.   Compliance during load-up to creep load, during unloading, and after fatigue at temperature for Test 12a.
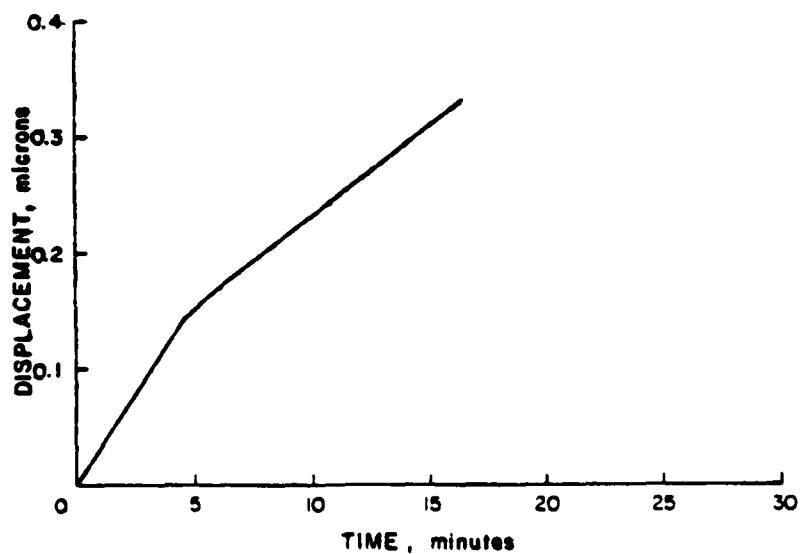
Figure 15.   Creep response at $K = 16.5$ MPa-m$^{\frac{1}{2}}$ for Test 12a.

The specimen was then fatigued at temperature for 5000 cycles at $K = 16.5$ MPa-m$^{\frac{1}{2}}$ at 730°C. The compliance shown in Figure 14 indicated crack growth. A new load for $K \cong 25.3$ MPa-m$^{\frac{1}{2}}$ was estimated, and another creep test run for 30 minutes. Figure 16 shows the loading and unloading compliances with the creep plotted in Figure 17.

Figure 16.   Compliances during load-up to creep load and during unloading for Test 12b.
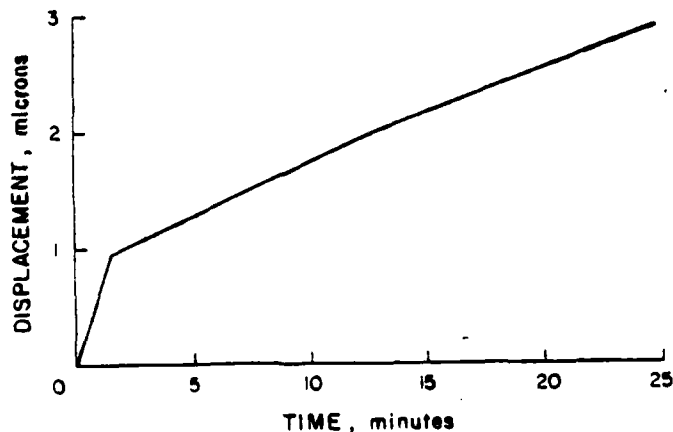
Figure 17.   Creep response at $K = 25.3$ MPa-m$^{\frac{1}{2}}$ for Test 12b.

The process was then repeated with the crack grown 5000 cycles at $K = 16.5$ and 1200 cycles at $K = 25.3$ MPa-m$^{\frac{1}{2}}$. Figure 18 has the loading-unloading and Figure 19 the creep.

22

Figure 18.   Compliances during load-up to creep load and during
unloading for Test 12c.

Figure 19.   Creep response at $K = 38.5$ MPa-m$^{\frac{1}{2}}$ for Test 12c.
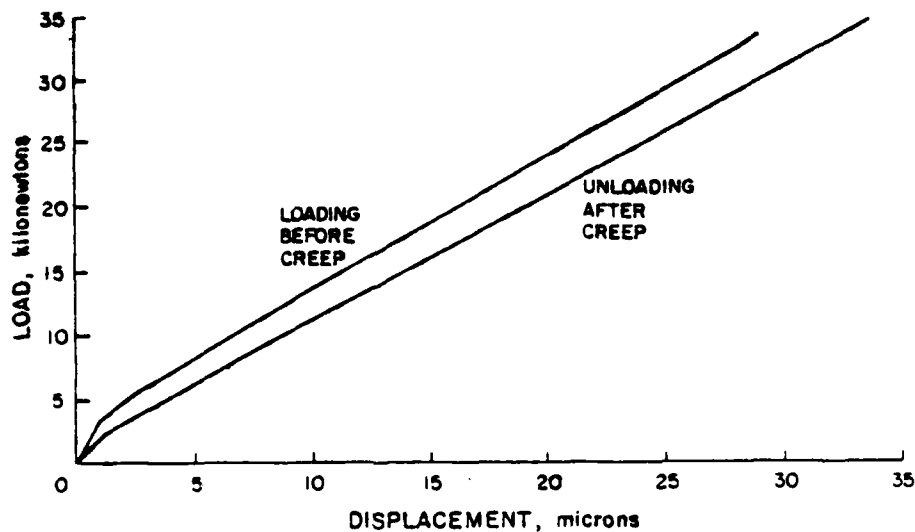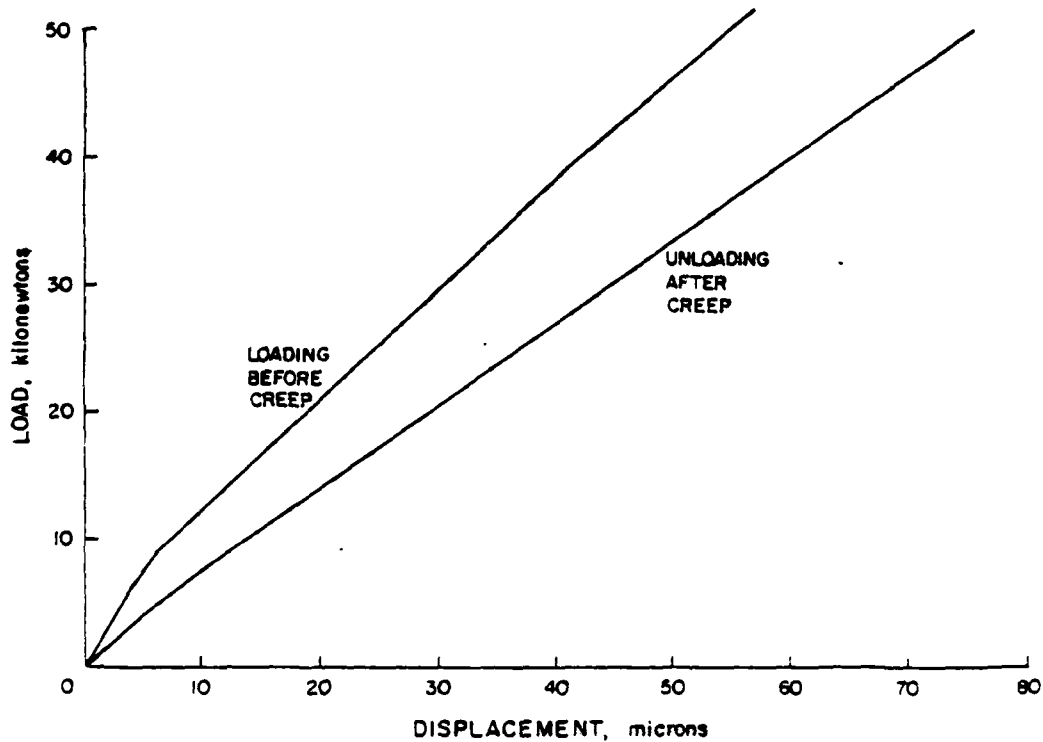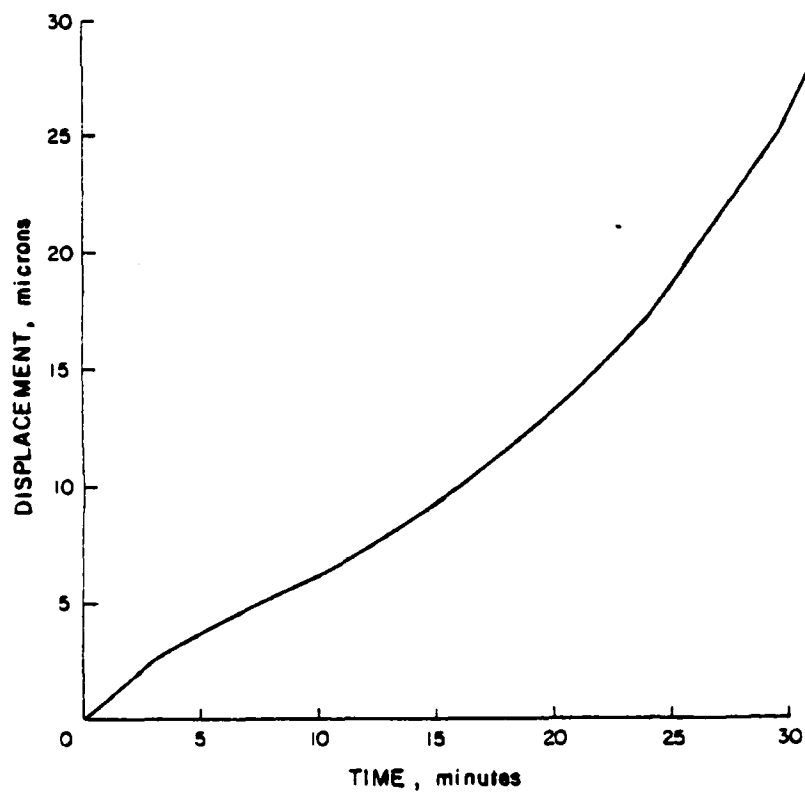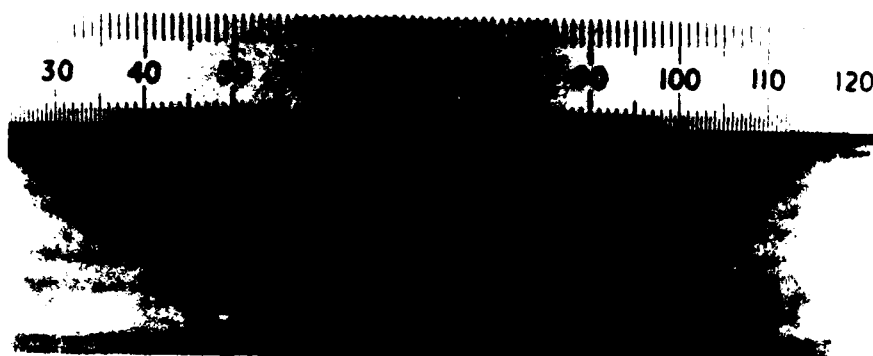
Figure 20 is a photograph of the fracture surface of Specimen 3 after testing. Note how curved the crack fronts are.

Specimen 3

Figure 20.   Photograph of specimen #3 after Test 12.

PHASE II RESULTS

Experiments in this later part of the program were similar to PHASE I except that a minicomputer was acquired and used to control the tests. Load is controlled from the minicomputer; it also records the fringe motions during each compliance.

The specimen was loaded to half the maximum load, and then the laser beam was adjusted so that the fringes would be visible when the maximum load was reached. Some initial load must be on the specimen prior to adjusting the laser - it is very difficult to start from zero load because of specimen movement in the grips. The minicomputer then controlled loading of the specimen to the maximum load, paused 2 seconds, and then ran the first compliance. Subsequent compliances are run on command from the keyboard; each compliance took 8 seconds.

For the first 7 tests (Nos. 21, 22, 24-28) in this phase, creep displacement was measured on the stripchart recorder and analyzed manually. Upon acquisition of FORTRAN capability (earlier programing was in BASIC), it was possible to store the creep data. The last two tests (Nos. 30, 31) were run using this approach.

A program was written to reduce the load-fringe data into load-displacement data. A straight line was fit using a least squares analysis, and almost all the data had a regression coefficient, R, better than 0.999. The compliance was computed for the last part of the initial loading; this is referred to as the compliance at t = 0.

Test Number - 21

Specimen Number - GC-2

Crack Length (mm)	Before	After
A	3.73	3.73
B	3.71	3.89
C	4.19	4.04 (measurement error)
D	3.71	3.84

Creep Load (kN) - 40.2   Compliance Increment (kN) - 4.95

Stress Intensity Factor (MPa-m$^{\frac{1}{2}}$) - 25.3   Temperature (C) - 732

Test Duration - 47 minutes

ISDG Location - 1.32 mm from centerline along crack B.

Table 1 lists the compliances and percent changes during creep; Figure 21 plots the displacement during creep.
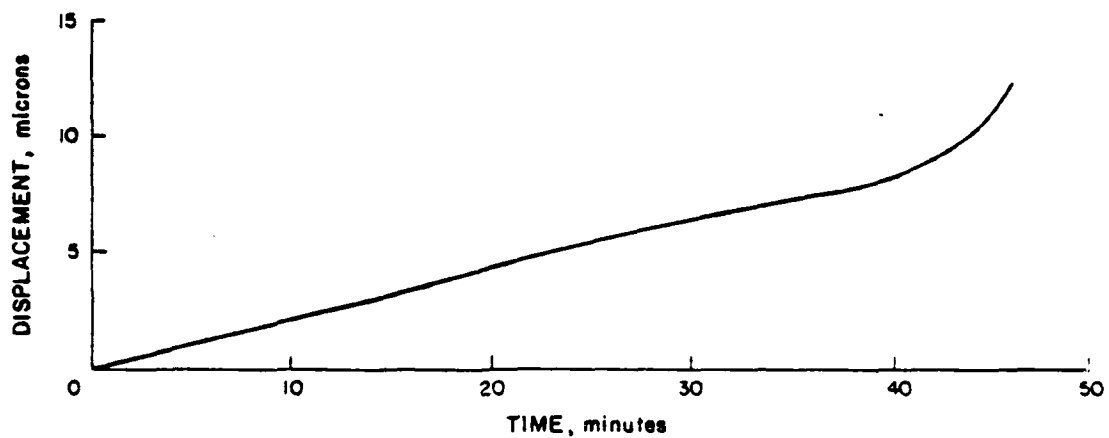
Figure 21.   Creep response for Test 21 at 40.2 MPa-m$^{\frac{1}{2}}$.

Table 1

t	a	Compl Unload	Compl Load	Avg Compl	% Change from Loading
min:sec	mm	$\mu m/Ntx10^{-4}$	$\mu m/Ntx10^{-4}$	$\mu m/Ntx10^{-4}$	
0	3.71	-	7.21	7.21	-
:02		6.68	6.61	6.64	-7.9
:16		6.68	6.86	6.77	-6.1
2:28		6.72	6.75	6.74	-6.5
5:30		6.80	6.86	6.83	-5.3
20:31		7.12	7.22	7.17	-0.6
35:37		7.74	7.51	7.62	+5.7
46:57	3.89	8.44	8.43	8.44	+17.1

27

Specimen Number - GC-1

Crack Length (mm)	Before	After
A	3.53	3.81
B	3.73	3.89
C	3.48	3.76
D	3.53	3.76

Creep Load (kN) - 67.3   Compliance Increment (kN) - 8.28

Stress Intensity Factor (MPa-m$^{\frac{1}{2}}$) - 38.5   Temperature (C) - 732

Test Duration - 12½ minutes

ISDG Location - 1.07 mm from centerline along crack D.

   Table 2 lists the compliance data, and Figure 22 shows the creep displacement.
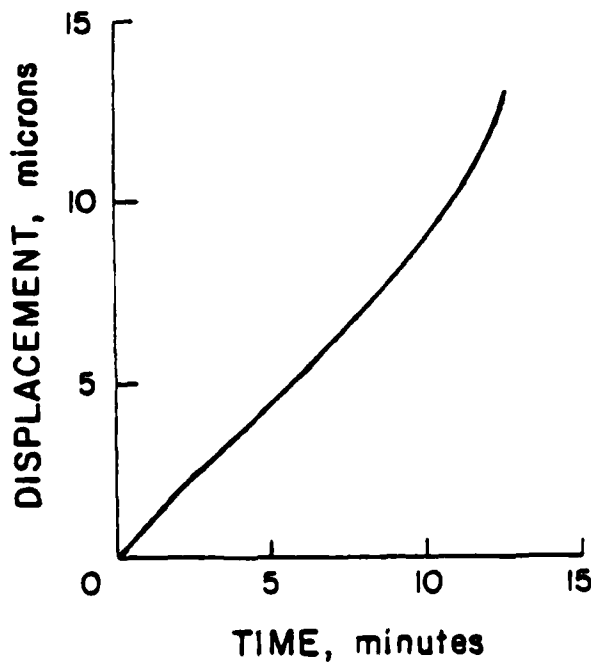
Figure 22.   Creep response for Test 22 at 38.5 MPa-m$^{\frac{1}{2}}$.

Table 2

t	a	Compl Unload	Compl Load	Avg Compl	% Change from Loading
min:sec	mm	$\mu m/Ntx10^{-4}$	$\mu m/Ntx10^{-4}$	$\mu m/Ntx10^{-4}$	
0	3.53	-	7.96	7.96	-
:02		6.60	6.74	6.67	-16.2
:30		6.64	6.71	6.68	-16.1
1:28		6.71	6.72	6.72	-15.6
3:51		6.92	6.87	6.88	-13.6
8:12		7.23	7.35	7.27	-8.7
12:28	3.76	7.71	7.71	7.71	-3.1

<u>Test Number</u> - <u>24, 25, 26</u>

Specimen Number - GC-1 (precracked at room temperature after Test 22)

Crack Length (mm)	Before
A	8.20
B	5.16
C	4.57
D	5.49

Creep Load (kN) - 47.4   Compliance Increment (kN) - 5.83

Stress Intensity Factor (MPa-m$^{\frac{1}{2}}$) - 38.5   Temperature (C) - 732

Test Duration - ~ 10 seconds, 5½ minutes, 10 seconds

ISDG Location - 1.07 mm from centerline along crack D.

A malfunction shut off the MTS machine shortly after the maximum load for Test 24 had been reached; therefore, only the first two compliances were recorded. These are given in Table 3.

The specimen was immediately reloaded for Test 25 and held at load for 5½ minutes. The compliances are given in Table 3 and the creep displacement in Figure 23. One channel of the fringe compliance data was bad during the loadup and first compliance. Test 26 is an immediate reload after Test 25, and compliances are given in Table 3.

Figure 23.   Creep response for Test 25 at 38.5 MPa-m$^{\frac{1}{2}}$.

Table 3

t	a	Compl Unload	Compl Load	Avg Compl	% Change from Loading
min:sec	mm	$\mu m/Ntx10^{-4}$	$\mu m/Ntx10^{-4}$	$\mu m/Ntx10^{-4}$	
0	5.49	-	12.2	12.2	-
:02		10.2	10.4	10.3	-16.6
Test 25					
0		-	11.7*	11.7*	-
:02		10.3*	10.9*	10.6*	-9.4
:43		10.7	10.8	10.8	-7.7
4:30		11.3	11.6	11.4	-2.6
5:30		Unloaded			
Test 26					
0		-	13.4	13.4	-
:02		11.6	12.2	11.9	-11.2

*Based on one channel.

<u>Test</u> <u>Number</u> - <u>27, 28</u>

Specimen Number - GC-3 (after additional precracking at room temperature)

Crack Length (mm)	Before
A	8.43
B	9.07
C	8.99
D	8.36

Creep Load (kN) - 20.2   Compliance Increment (kN) - 2.49

Stress Intensity Factor (MPa-m$^{\frac{1}{2}}$) - 25.3   Temperature (C) - 732

Test Duration - 23.5 minutes, 10 seconds

ISDG Location - 1.32 mm from centerline along crack C.

Test 27 was a creep test at 25.3 MPa-m$^{\frac{1}{2}}$ - similar to Test 21 except that the crack is a lot longer. Compliance data is given in Table 4 with the creep displacement in Figure 24. Test 28 was an immediate reload with the first compliance.
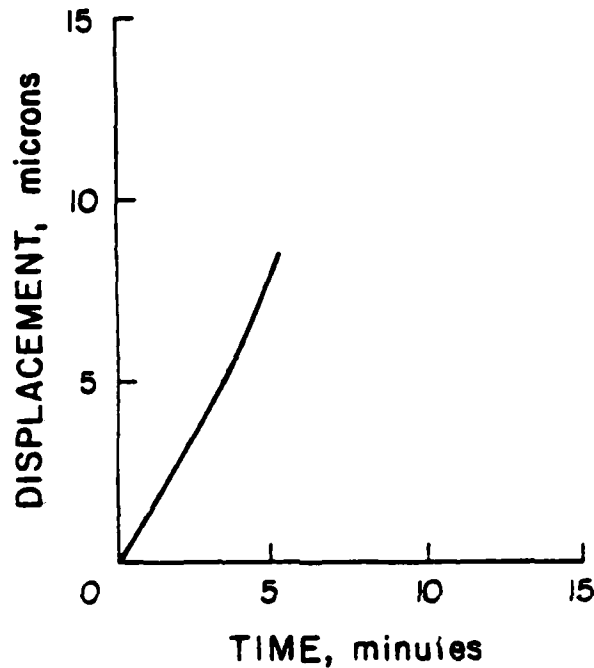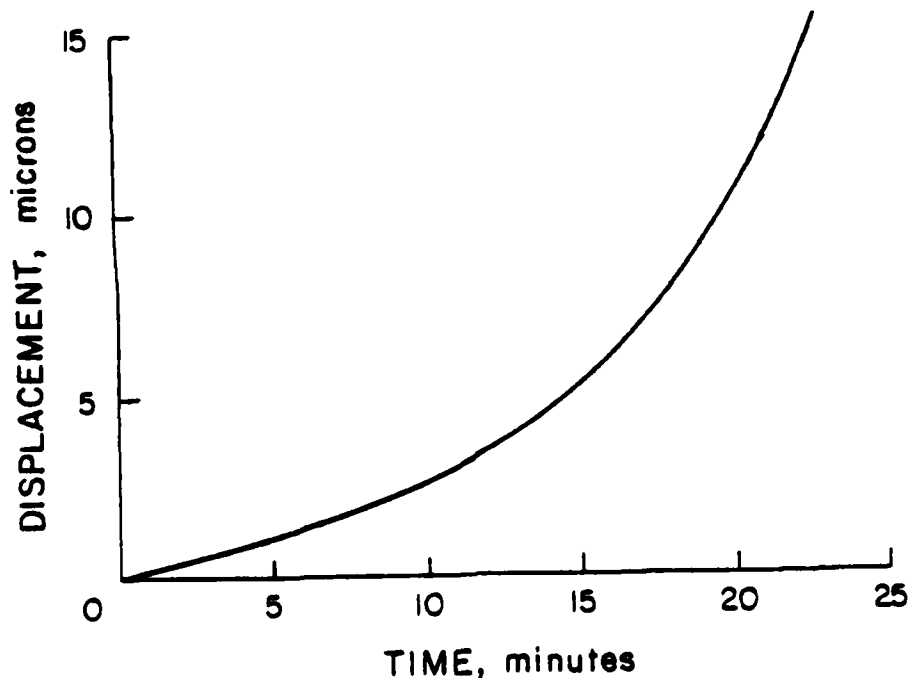

Figure 24.   Creep response for Test 27 at 25.3 MPa-m$^{\frac{1}{2}}$.

32

Table 4

t	a	Compl Unload	Compl Load	Avg Compl	% Change from Loading
min:sec	mm	$\mu m/Ntx10^{-4}$	$\mu m/Ntx10^{-4}$	$\mu m/Ntx10^{-4}$	
Test 27					
0	8.99	-	20.3	20.3	-
:02		19.5	19.7	19.6	-3.4
2:13		10.3	19.6	20.0	-1.5
5:15		20.3	19.5	19.9	-2.0
10:19		21.7	20.5	21.1	+3.9
20:44		23.2	23.2	23.2	+14.3
23:19		26.2	24.4	25.3	+24.6
Test 28					
0		-	30.6	30.6	-
:02		25.3	26.8	26.0	-15.0

<u>Test</u> <u>Number</u> - <u>30</u>

Specimen Number - 1 (after additional precracking at room temperature)

<u>Crack Length (mm)</u>	<u>Before</u>
A	4.39
B	4.53
C	3.62
D	3.67

Creep Load (kN) - 61.7   Compliance Increment (kN) - 7.4

Stress Intensity Factor (MPa-$m^{\frac{1}{2}}$) - 38.5   Temperature (C) - 732

Test Duration - 27 minutes

ISDG Location - 2.37 mm from centerline along crack D.

    The compliance data for Test 30 are given in Table 5; they are consistent with the data in Table 2 which is for a crack of similar length at the same maximum K. One of the objectives on this test was to take frequent compliance measurements to demonstrate reproducibility. All the compliances in the first 5 minutes are virtually identical. The creep data is given in Figure 25; it too is consistent with Figure 22.

Figure 25.   Creep response for Test 30 at 38.5 MPa-m$^{\frac{1}{2}}$.

35

Table 5

t	a	Compl Unload	Compl Load	Avg Compl	% Change from Loading
min:sec	mm	$\mu m/Ntx10^{-4}$	$\mu m/Ntx10^{-4}$	$\mu m/Ntx10^{-4}$	
0	3.67	-	8.06	8.06	-
0:02		5.85	6.06	5.96	-26.1
0:31		6.04	6.01	6.02	-25.3
2:00		6.10	6.08	6.09	-24.4
2:08		6.09	5.94	6.02	-25.3
5:01		6.01	6.17	6.09	-24.4
10:02		6.47	6.48	6.48	-19.6
25:02		7.66	7.60	7.63	- 5.3

<div align="center"><u>Test</u> <u>Number</u> - <u>31</u></div>

Specimen Number - GC-4

Crack Length (mm)	Before
A	3.48
B	3.61
C	3.88
D	3.43

Creep Load (kN) - 28.9   Compliance Increment (kN) - 3.55

Stress Intensity Factor (MPa-m$^{\frac{1}{2}}$) - 16.5   Temperature (C) - 732

Test Duration - 3 hours

ISDG Location - 1.32 mm from centerline along crack B.

Compliance data are given in Table 6 and creep response in Figure 26. These data show more scatter than usual because the low compliance increment produced only 1 to 1½ fringe motions. However, the same trend is shown as in other results. Creep displacment is observed even for such a low K.
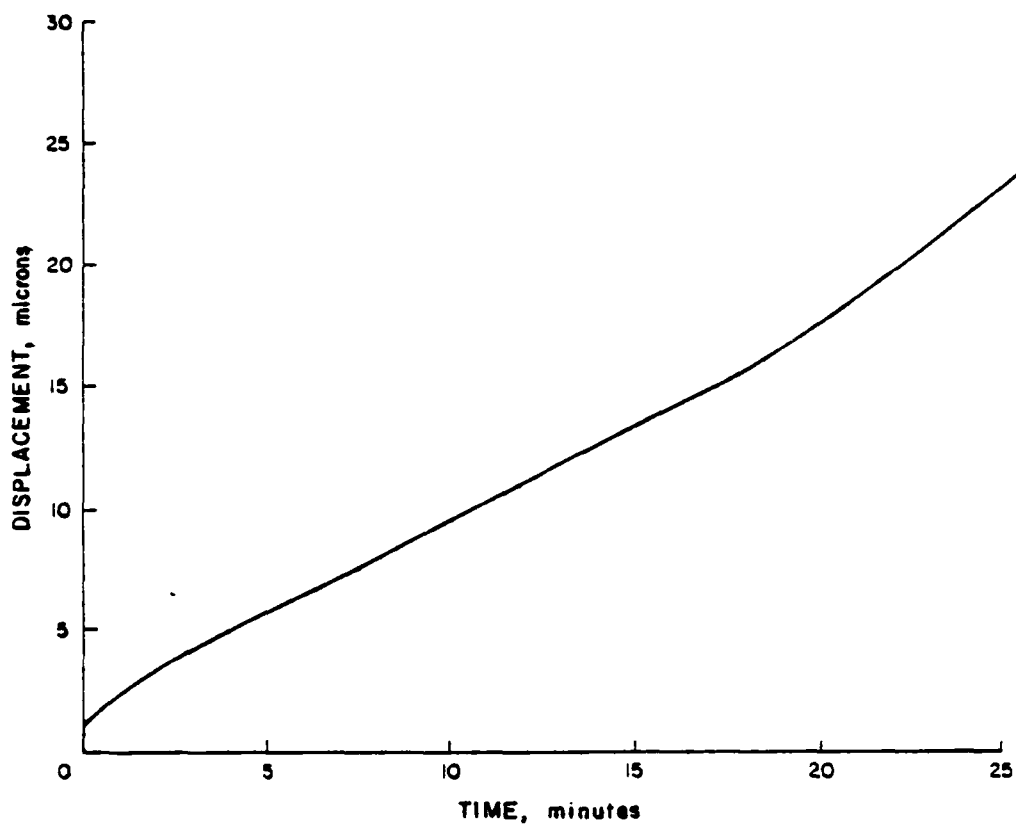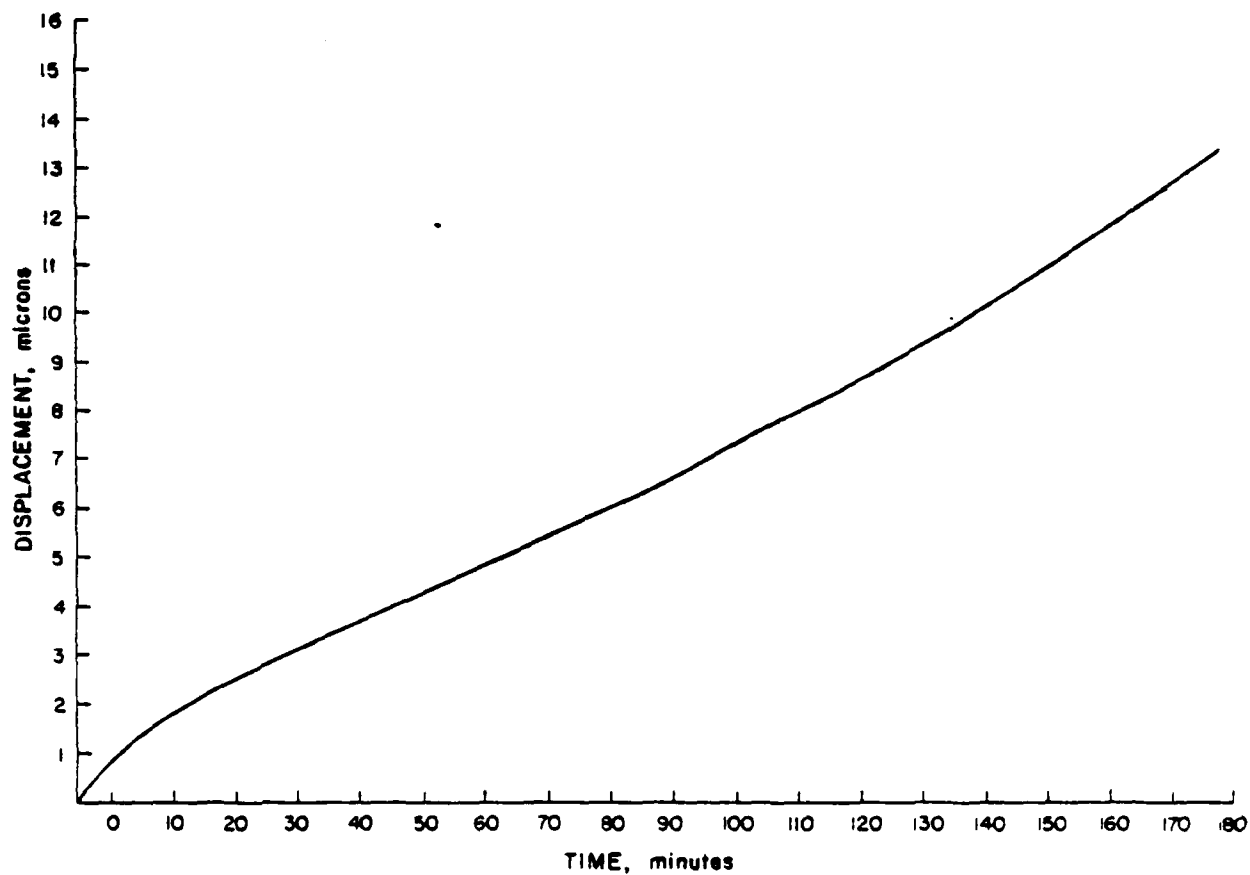
Figure 26.   Creep response for Test 31 at 16.5 MPa-m$^{\frac{1}{2}}$.

Table 6

t	a	Compl Unload	Compl Load	Avg Compl	% Change from Loading
hr:min:sec	mm	$\mu m/Ntx10^{-4}$	$\mu m/Ntx10^{-4}$	$\mu m/Ntx10^{-4}$	
0	3.61	-	6.33	6.33	-
0:02		6.10	5.93	6.01	- 5.1
0:35		6.39	6.07	6.23	- 1.6
2:01		6.21	6.06	6.14	- 3.0
5:04		6.02	6.37	6.20	- 2.1
15:56		6.06	6.10	6.08	- 3.9
29:58		6.37	6.42	6.40	+ 1.1
45:04		6.39	6.48	6.44	+ 1.7
1:01:48		6.63	6.49	6.56	+ 3.6
1:16:41		6.84	6.48	6.66	+ 5.2
1:31:13		6.70	6.90	6.80	+ 7.4
1:31:13		6.70	6.90	6.80	+ 7.4
1:46:12		7.18	7.06	7.12	+12.5
2:02:02		7.26	7.19	7.22	+14.1
2:15:23		7.70	7.56	7.63	+20.5
2:30:31		7.63	7.49	7.56	+19.4
2:45:05		8.15	8.14	8.14	+28.6
2:50:14		8.46	8.14	8.30	+31.1

CONCLUDING REMARKS

Displacement measurements at high temperatures are difficult at best, and especially so over a short gage length. The ISDG technique has been shown to work quite well for this particular superalloy and temperature, i.e. the fringes stay bright permitting longer term measurements.

This report is in a sense a chronicle of the development of the experimental techniques associated with creep and compliance testing at high temperature and the associated ISDG data acquisition and analysis. The work started with manual control of loading/compliance and manual data analysis of the ISDG strip chart records. It ended with mini-computer control of loading/compliance and minicomputer-based data analysis. The last two tests (Nos. 30 and 31) used the final version of the system. Most of the experiments used fixed mirrors with a resolution of approximately 1/8 micron and a relative uncertainty of ± 3 percent.

The displacement measurement setup is very simple - a laser, 2 PMTs, and a small minicomputer. However, the more sophisticated system using servocontrolled mirrors which is described in reference 3 has the advantage of a resolution on the order of 1/50 micron.

Creep tests with the good resolution described herein can be used to establish threshold values on an accelerated basis. It is clear (Figure 26) that the threshold value is less than 16.5 MPa-m$^{\frac{1}{2}}$.

The change in compliance with time at load and at temperature are demonstrated in the Tables. The compliance immediately after reaching maximum load is smaller - indicating a stiffer specimen. Figure 27 gives a better view of the results for Test 30. As the specimen is loaded initially (the starting load was 0.18 KN), its behavior is linear with a compliance of 6.13×10^{-4} μm/Nt. At higher loads, the behavior becomes nonlinear due to plastic deformation around the crack tip, and a higher compliance is observed. The compliance was run 2 seconds after reaching the maximum load is 5.96×10^{-4} μm/Nt which is within 3 percent of the initial value. The specimen again behaved elastically, and there was no crack growth. The behavior shown in this first part of Figure 27 is similar to that observed in simple tension testing into the plastic region with a partial loading cycle.
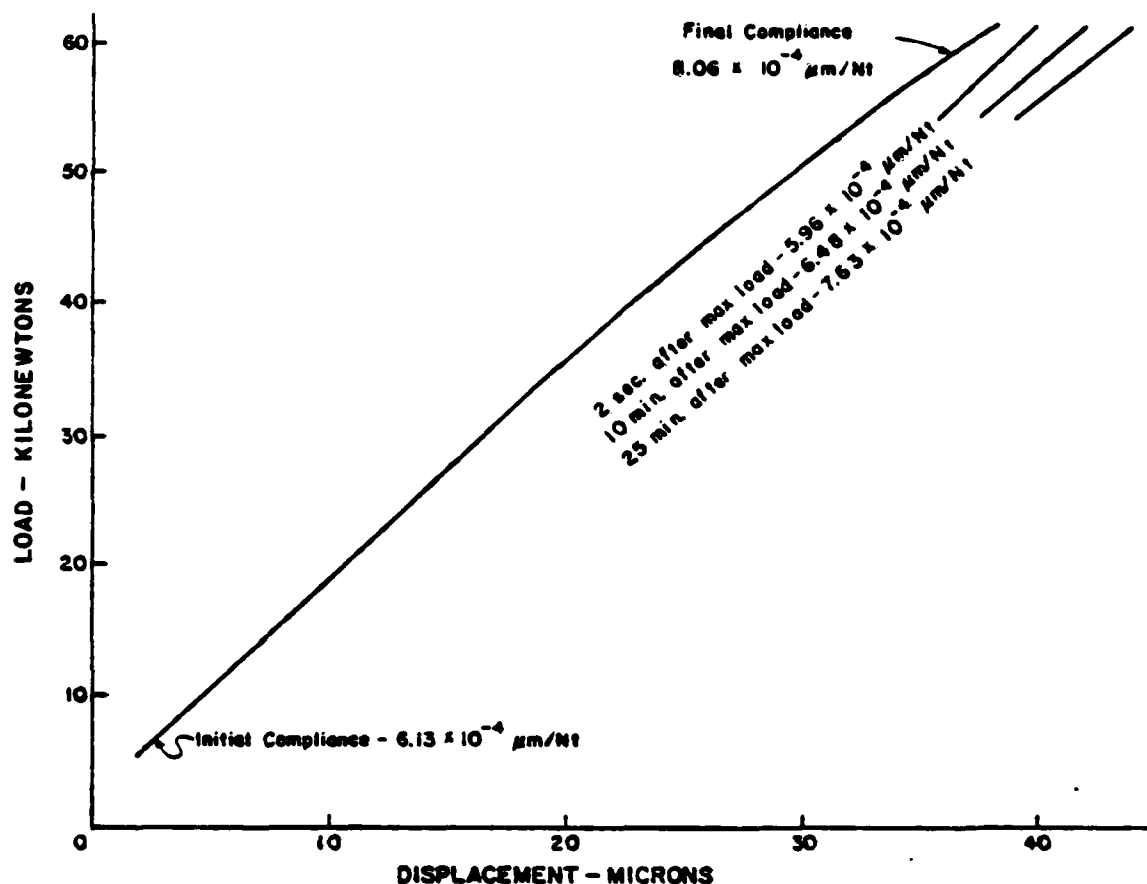
Figure 27.   A plot of the total load-displacement response for
              test 30 and three subsequent compliance measurements.

Changes in the compliances at later times indicate crack growth. A
recent study (5) has used a nonlinear finite element code to predict
crack growth from displacement measurements. The results in Phase I
was used by those authors.

In closing then, the experimental techniques described in this
report have been shown to be capable of establishing material behavior
directly, e.g. creep threshold values. But they can also be used to
generate data which can be used indirectly - via finite element codes -
to determine material behavior. These measurement capabilities under
high temperature conditions may be quite useful in furthering the under-
standing of cracked components subjected to severe conditions.

REFERENCES

1. Sharpe, W. N., Jr., "Interferometric Surface Strain Measurement,"
   International Journal of Nondestructive Testing, Vol. 3, pp. 59-76,
   1971.

2. Macha, P. E., Sharpe, W. N., Jr., and Grandt, A. E., Jr., A Laser
   Interferometry Method for Experimental Stress Intensity Factor
   Calibration," ASTM STP601, pp. 490-505, 1976.

3. Domas, P. A., Sharpe, W. N., Jr., Ward, M., and Yau, J., "Benchmark
   Notch Test for Life Prediction," NASA Report CR-165571, 220 pgs.,
   1982.

4. Donath, R. C., Nicholas, T., and Fu, L. S., "An Experimental Inves-
   tigation of Creep Crack Growth in IN-100," ASTM STP743, pp. 186-206,
   1981.

5. Hinnerichs, T. D., "Viscoplastic and Creep Crack Growth Analysis by
   the Finite Element Methods," AFWAL-TR-80-4140, Wright-Patterson
   AFB, Ohio, 1980.

ATE
LME